

FAILURE CASE STUDY SERIES PART THREE: INVESTIGATION OF WEAR AND FAILURE MECHANISMS IN HEAVY-DUTY GEAR COUPLING

Liviu GURĂU, Florin MARIN, Mihaela MARIN, Cristian ȘTEFĂNESCU,
Gheorghe GURĂU*

Interdisciplinary Research Centre in the Field of Eco-Nano Technology and Advanced Materials CC-ITI,
Faculty of Engineering, "Dunarea de Jos" University of Galati, 47 Domneasca Street, 800008 Galati, Romania
e-mail: gheorghe.gurau@ugal.ro

ABSTRACT

This paper investigates the failure mechanisms of the gear teeth in a heavy-duty coupling, emphasizing the combined effects of mechanical loading, metallurgical microstructure, and tribological wear mechanisms.

Detailed characterization using optical microscopy (OM), scanning electron microscopy (SEM), energy-dispersive X-ray spectroscopy (EDS), and both chemical and mechanical testing identified pronounced wear and progressive degradation of the coupling sleeve, largely driven by operational misalignments and external contamination, such as mill cobbles. The analysis underscores the critical importance of precise material compatibility, a controlled hardness differential, and manufacturing accuracy in mitigating localized stress concentrations and wear. The findings highlight that abnormal wear progression results from a complex interaction among load redistribution owing to misalignment, tribological deterioration, manufacturing tolerances, and dynamic rotor-coupling interactions. Recommendations focus on optimizing design parameters, manufacturing processes, and operational routines to enhance the reliability, durability, and safety of high-torque coupling systems in harsh industrial environments.

KEYWORDS: failure analysis, gear-coupling, OM, SEM, EDS

1. Introduction

This paper presents a comprehensive analysis of the failure mechanisms observed in the gear teeth of a coupling used within a rolling mill assembly. The coupling exhibited pronounced abnormal wear patterns and progressive tooth damage-phenomena closely associated with mill cobble contamination. Gear couplings are indispensable in high-torque transmission systems operating under strenuous conditions; where the mechanical integrity of the gear teeth determines overall system reliability and safety. Deterioration phenomena such as wear, pitting, and crack initiation, compromise torque transfer efficiency; induce operational instability; and elevate the risk of unplanned downtime, or secondary damage to mill components [1, 2].

The investigation involved a visual assessment and advanced metallurgical examinations of the failed coupling components, emphasizing the interaction between material properties and operational stresses.

The coupling configuration comprises hubs attached to the motor and gear shafts interconnected through internal sleeves. Typically, hubs are fabricated from high-strength alloy steels to resist fatigue and high-torque loads; conversely, sleeves are constructed from wear-resistant or case-hardened steels designed to withstand sliding contact, misalignment, and cyclic loading [3, 4].

A key factor influencing coupling life is the metallurgical relationship between the materials used for both the hub and the sleeve. An optimal hardness differential - ideally with the sleeve ideally slightly harder than the hub - ensures balanced wear and mitigates excessive tooth wear, pitting, or failure [5]. An imbalance where one component is significantly harder or softer accelerates localized wear and may lead to fatigue cracking at the tooth roots or edges [6]. Such relationships must be precisely engineered and monitored to optimize tribological compatibility.

From a geometric perspective, the contact of the straight internal teeth with the external teeth on the

hub is designed to accommodate misalignment and facilitate sliding during operational angular displacement. While crowned or spherical external teeth have been employed in some coupling applications to improve contact conformity, the external gear teeth in this study are straight, with the design optimized for specific misalignment conditions. Even minor offsets can significantly influence meshing forces and contact patterns, as evidenced by finite element and analytical studies [7, 8]. These misalignments often lead to an uneven load sharing among the teeth, concentrating stresses toward the extremities of the gear teeth and thereby promoting fatigue and crack initiation at the root fillets [9].

Furthermore, manufacturing precision plays an essential role in load distribution during misaligned operation. Properly controlled manufacturing processes enhance interface conformity, reducing stress concentrations and prolonging gear service life [10, 11]. Deviations or inaccuracies in tooth geometry can accentuate load unevenness, thereby increasing wear and the likelihood of failure.

Tribological performance, particularly lubricant film stability, directly impacts wear progression. Under angular misalignment, contact migration toward tooth edges intensifies sliding and frictional heating, risking film collapse and surface wear [12, 13]. Lubricant selection, surface finish, and maintenance are critical in mitigating these effects. When a small number of teeth bear disproportionate loads due to misalignment, localized roughening, micropitting, and abrasion are amplified, decreasing the durability of the gear teeth [14].

The abnormal wear and progressive damage observed in the coupling teeth derive from a complex interaction of mechanical, metallurgical, geometric,

and tribological factors. Addressing these issues requires an integrated approach encompassing precise manufacturing, proper material selection, lubrication management, and real-time operational monitoring. These measures are essential to ensure the longevity and safe operation of heavy-duty couplings in demanding industrial environments.

2. Experimental procedure

The failure investigation adhered to the protocol outlined in our previous study [15]. This involved determining the chemical composition of the components; examining the fracture morphology through stereomicroscopy; and performing an in-depth microstructural and surface-damage assessment using OM, SEM, and EDS techniques [15]. Furthermore, the mechanical behavior of the material was evaluated via hardness measurements.

The investigations were conducted on both the hub and sleeve of the gear coupling (Figure 1).

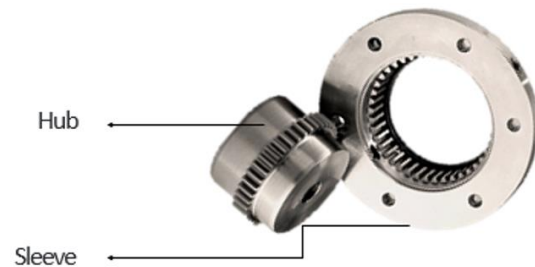


Fig. 1. Gear coupling

The recommended materials for this coupling are presented in Table 1.

Table 1. ASTM equivalents of the recommended steel grades

Steel Type	Grade	ASTM Grades	Key Properties	Typical Applications
Chromium-Molybdenum Alloy	AISI 4140	ASTM A29 Grade 4140 (for forgings), ASTM A322 / A322M (bars)	High strength, toughness, good hardenability, suitable for heat treatment	Medium to heavy-duty mechanical components, gear couplers, shafts, and gears
Nickel-Chromium-Molybdenum Alloy	AISI 4340	ASTM A29 Grade 4340	Very high toughness, excellent fatigue resistance, high hardenability	Heavy-duty gear couplings, high-load shafts, critical mechanical parts
Medium Carbon	AISI 1045 / 1050	ASTM A36 / AISI 1045	Moderate strength and hardness; can be surface-hardened (carburized or induction hardened)	Light to medium-load couplers, shafts, general mechanical components

3. Results and discussion

3.1. Chemical composition

Samples were taken separately from the sleeve and the hub for spectral analysis to determine their material composition. The results of the analysis are presented in Table 2. This examination helps verify whether the materials meet the required specifications

and identifies any anomalies that could have contributed to the failure. Understanding the chemical composition is crucial for assessing material properties and suitability for the application.

Using spark atomic emission spectrometry [15], we detected the chemical composition for both components as presented in Table 2.

Table 2. Chemical composition

Element	Sample A- Hub	Sample B- Sleeve
Carbon (C)	0.558	0.411
Silicon (Si)	0.224	0.306
Manganese (Mn)	0.645	0.664
Phosphorus (P)	0.012	0.009
Sulfur (S)	0.014	0.0025
Nitrogen (N)	0.0082	0.007
Chromium (Cr)	0.07	0.051
Molybdenum (Mo)	0.008	0.003
Nickel (Ni)	0.031	0.029
Calcium (Ca)	0.0013	0.0028
Aluminum (Al)	0.0162	0.025
Vanadium (V)	0.0014	0.0016
Titanium (Ti)	0.0009	0.0014
Copper (Cu)	0.048	0.046
Niobium (Nb)	0.0006	0.0011
Boron (B)	0.0002	0.00015
Iron (Fe)	98.356	98.433
CEV	0.6863	0.5375

We found that for this chemical composition, medium-carbon grades equivalent to AISI 1055 (C55 EN 10277-2-2008) for the hub and AISI 1040 (C40 (1.0511): EN 10277-2-2008) for the sleeve were used. Consequently, we observe a very large hardness/strength mismatch (Table 3) between the hub (C55) and the sleeve (C40). This mismatch could drive accelerated wear during normal torque transmission. Even if the design intent is to use the sleeve as a sacrificial element, the actual hardness gap

is too high, which led to rapid wear and a rapid catastrophic failure when torque and misalignment increased (the design aspects of the sacrificial sleeve concept need to be correlated with these results).

A practical pairing recommendation in the case of a sacrificial sleeve concept (controlled) is: Hub: ~300–340 HB; Sleeve: ~270–310 HB ($\approx -15-30$ HB vs. hub), with strict lubrication control and inspection intervals.

Table 3. HB [MPa] for both C40 EN 10277-2-2008 (sleeve) and C55 EN 10277-2-2008 (hub)

A) As-rolled / As-forged (no heat treatment):		B) Quenched & Tempered:	
C40	170–205 HB	C40	180–220 HB (soft temper) up to 35–45 HRC
C55	190–235 HB	C55	200–260 HB (soft temper) up to 50–56 HRC

3.2. Hardness test

The test method used for the gear sample pieces analysed (Figure 2) was Vickers Hardness (HV30) – ASTM E92 standard. The values were converted to HB (Brinell) and HRB (Rockwell) as well. The evaluation was conducted on the tooth-tip region as well as the core regions of both the hub and sleeve samples. The purpose was to confirm whether similar materials are used for the hub and sleeves and to identify hardness differences, if any.

Sample A (Hub) exhibits slightly higher hardness values at both the tooth tip (233 HV30) and core (234 HV30) compared to Sample B (Sleeve), which shows hardness values of 212 HV30 at the tooth tip and 220 HV30 at the core. This indicates that the hub material is marginally harder than the sleeve, which is consistent with its higher carbon content (Figure 3).

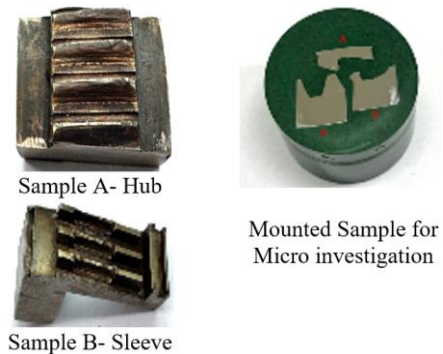


Fig. 2. Samples for hardness investigation (A) hub (B) sleeve

The lower hardness in the sleeve suggests it has comparatively less wear resistance, which likely contributed to the severe abrasive wear and tooth failure observed in the sleeve. Additionally, the small hardness difference between the tooth tip and core in the sleeve indicates a lack of surface hardening, making the teeth more vulnerable to wear under high contact stresses.

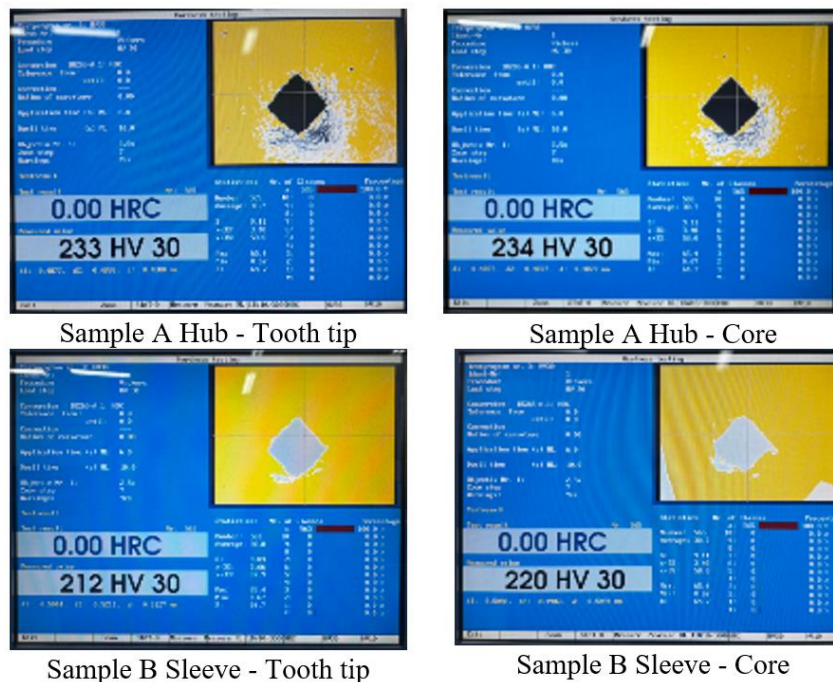


Fig. 3. Vickers hardness for hub and sleeve

3.3. Optical microscopy

As stated previously [15], the cross-sectional sample was polished up to 1500-grit emery grade, followed by 1 μm velvet cloth polishing, and then

etched using a 2% nital solution to reveal microstructures and observe defects. Micro-examination was carried out as per ASTM E407 and the ASM Handbook, Volume 9.

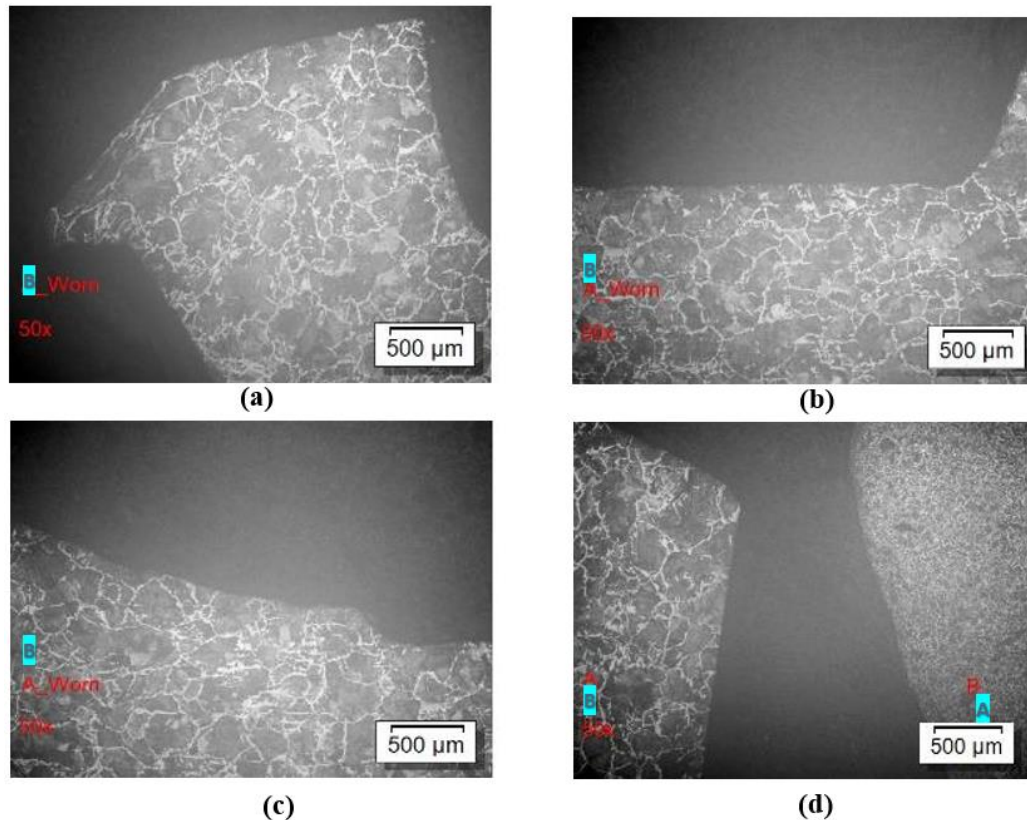


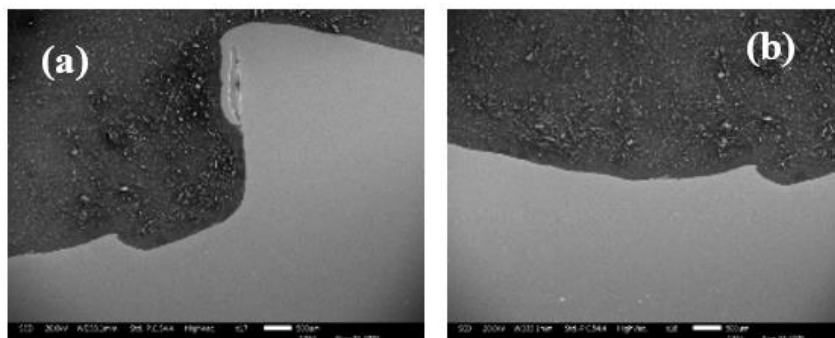
Fig. 4. OM microstructures: (a) Sleeve sample: Tooth tip regions did not reveal any hard microstructure, indicating no case hardening was applied; (b) Sleeve sample: Tooth-damage region showing a normal ferrite-pearlitic microstructure; (c) Sleeve sample: Tooth-damage region showing a normal ferrite-pearlitic microstructure; (d) Both samples' microstructure are ferrite-pearlitic. Hub Sample (A) shows significantly finer structure

Both the hub (Sample A) and sleeve (Sample B) show ferrite-pearlite microstructures, indicating that both components were produced from plain carbon steel or similar low-alloy steel. The hub sample exhibited a significantly finer microstructure compared to that of the sleeve sample.

No evidence of case hardening was observed in either the tooth tips or tooth damage regions. Both samples exhibit microstructures consistent with non-surface-hardened steels.

3.4. Scanning electron microscopy (SEM) and energy-dispersive X-ray spectroscopy (EDS)

For this study, a JEOL IT 300LV scanning electron microscope equipped with a Bruker energy dispersive X ray spectroscopy (EDS) detector was utilized.



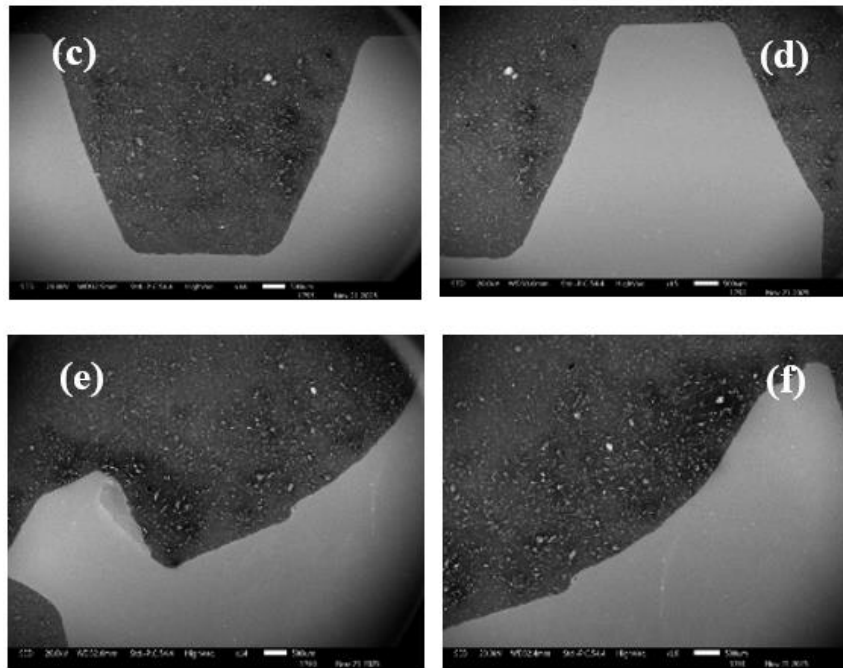
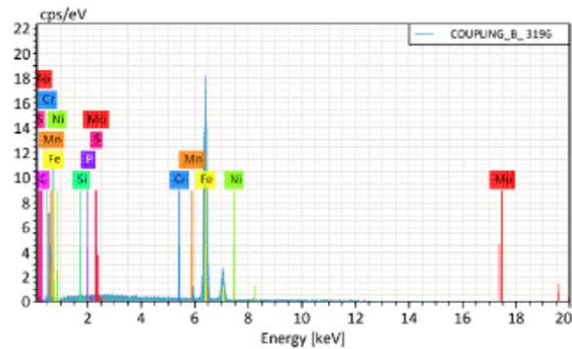
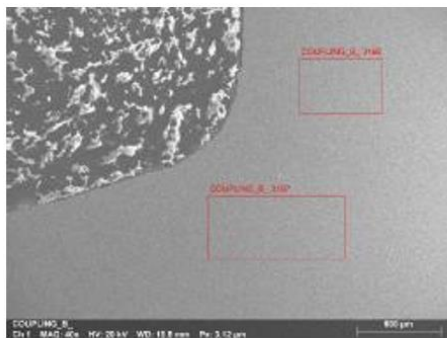


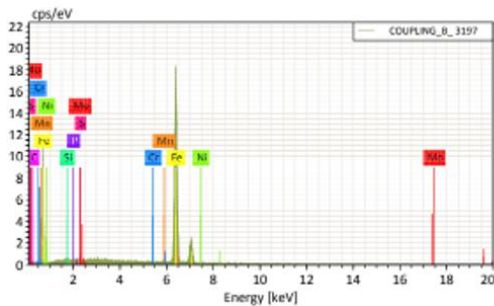
Fig. 5. SEM micrographs; (a) Hub -A Tooth region; (b) Hub-A worn out region; (c) Sleeve B tooth region; (d, e, f) Sleeve-B worn region

No material-related abnormalities were observed in the SEM (Figure 5) examination of either the hub or the sleeve. The worn regions showed no

inclusions, defects, or compositional anomalies, confirming that the material quality did not contribute to the observed damage.



EDS analysis



Spectrum	C	Si	P	S	Cr	Mn	Fe	Ni	Mo
COUPLING_B_3196	4.33	0.14	0.02	0.00	0.05	0.41	94.63	0.22	0.20
COUPLING_B_3197	3.61	0.30	0.01	0.00	0.00	0.42	95.65	0.00	0.01

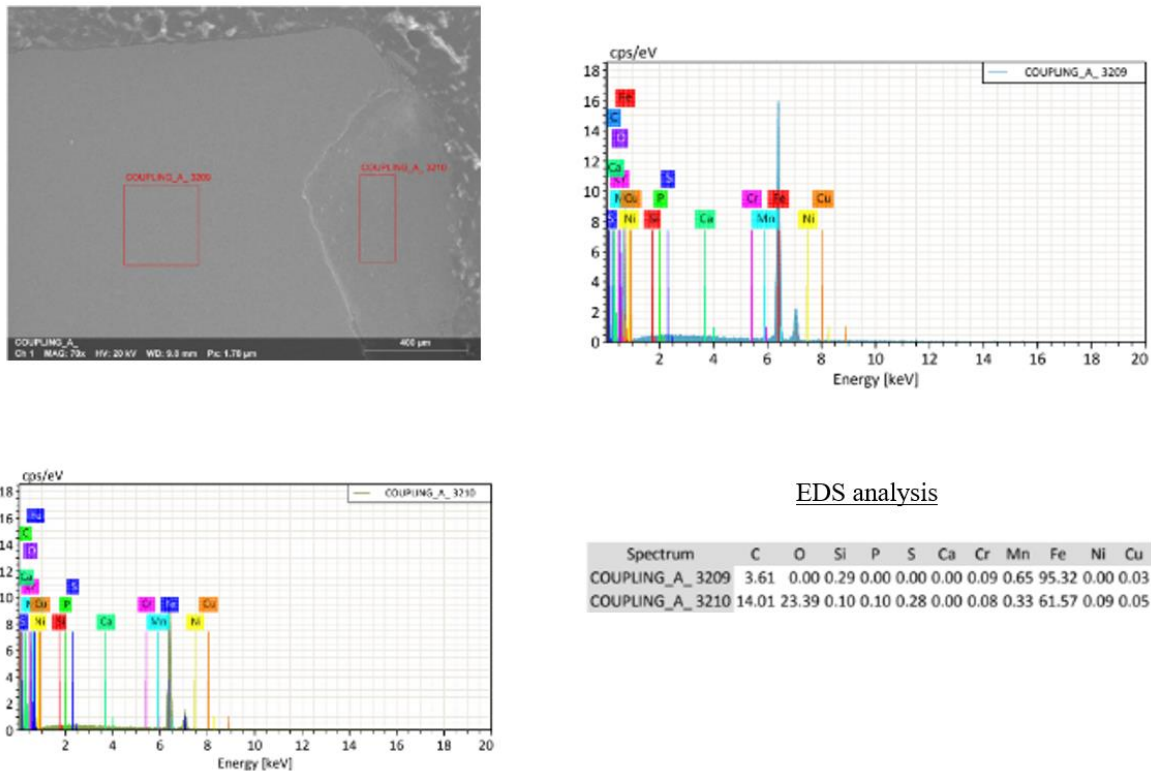


Fig. 6. EDS spectra on both sleeve and hub tooth

The EDS results closely match the measured chemical composition, confirming that the material was manufactured according to standard conditions and did not play a significant role in the coupler’s failure.

4. Conclusions

The thorough investigation into the failure of the hub and sleeve gear coupler, including visual inspection, hardness testing, chemical analysis, metallography, and SEM/EDS, provides insight into the mechanisms responsible for the sleeve tooth damage. All findings consistently indicate that the failure was driven by rapid, progressive abrasive wear, resulting from an excessive difference in hardness and strength between the hub and the sleeve. Importantly, no material-related abnormalities or microstructural defects were identified in either component.

Physical and microscopic examinations showed that the sleeve tooth wear was concentrated over approximately half of the available tooth width, demonstrating uneven load distribution during operation. The reduced load-bearing contact area accelerated tooth profile degradation under service conditions.

Chemical composition analysis confirmed that both the hub and sleeve were manufactured from

basic-medium carbon steels with an excessive difference between the grades. The sleeve exhibited lower carbon content without alloying elements compared to the hub. This difference resulted in lower achievable hardness and reduced wear resistance for the sleeve material.

Hardness measurements confirmed low and uniform bulk hardness across both the hub and sleeve teeth, with no hardness gradient and no indication of carburizing or induction hardening. This lack of surface hardening severely limited wear resistance under high-torque, cyclic loading.

Metallography revealed normal ferrite–pearlite microstructures throughout all examined regions. However, the hub sample exhibited a significantly finer microstructure compared to the sleeve. This observation is in line with the damage found in the sleeve. No evidence of case hardening, abnormal transformation products, cracking, or other microstructural abnormalities was observed. SEM/EDS analysis further confirmed the absence of inclusions, defects, or compositional anomalies in the worn regions.

We conclude that the root cause of the failure can be conclusively attributed to the combined influence of the hub–sleeve chemistry disparity (lower-carbon sleeve), the associated reduction in sleeve hardness, and an uneven tooth-width load distribution. These factors acted synergistically to

accelerate wear and precipitate premature failure under service torque. Metallurgical evidence also confirms that the absence of required surface hardening and the inherently softer, lower-carbon sleeve material led to progressive abrasive wear, tooth profile loss, and the final functional failure of the gear coupling.

References

- [1]. Lin Z., et al., *Dynamic characteristics of the gear coupled rotor system with both bearing defect and coupling misalignment*, *Nonlinear Dynamics*, 113, p. 25683-25713, 2025.
- [2]. Miao X., et al., *Dynamic characteristics of rotor system with parallel and angular misaligned involute spline coupling*, *Meccanica*, 59, p. 1061-1085, 2024.
- [3]. Wang J., et al., *An accurate finite element model for tooth contact and meshing force distribution of crown gear coupling*, *Journal of Mechanical Science and Technology*, 39(5), p. 2767-2778, 2025.
- [4]. Zhang C., et al., *An improved dynamic model of the spline coupling with misalignment and its load distribution analysis*, *International Journal of Mechanics and Materials in Design*, 20, p. 393-408, 2024.
- [5]. Jangra D., et al., *Gear sliding wear: The role of radial, axial, and combined misalignment*, *Journal of Mechanical Science and Technology*, 39, p. 5375-5383, 2025.
- [6]. Zhao Y., et al., *A lubrication contact pair model for simulating gear micro pitting damage characteristics based on contour integral*, *Advances in Mechanical Engineering*, 13(8), p. 1-9, 2021.
- [7]. Li Z., et al., *Nonlinear dynamics of unsymmetrical rotor bearing system with fault of parallel misalignment*, *Advances in Mechanical Engineering*, 10(5), p. 1-17, 2018.
- [8]. Wang J., et al., *Finite element analysis of gear tooth root crack under misalignment*, *The Journal of Engineering*, (In press), <https://doi.org/10.1049/joe.2018.9209>, 2025.
- [9]. Iñurritegui A., et al., *Spherical gear coupling design space analysis for high misalignment applications*, *Mechanism and Machine Theory*, 173, 104837, 2022.
- [10]. Guan Y., et al., *Clearance distribution and contact characteristics considering hob feed path in misaligned gear couplings*, *Scientific Reports*, 15, p. 1-16, 2025.
- [11]. de Bechillon N. G., et al., *A new experimental methodology to assess gear scuffing initiation*, *Tribology-Materials, Surfaces & Interfaces*, 16(3), p. 245-255, 2022.
- [12]. Jangra D., et al., *Gear sliding wear: The role of radial, axial, and combined misalignment*, *Journal of Mechanical Science and Technology*, 39, p. 5375-5383, 2025.
- [13]. Olson R., et al., *Case study of ISO/TS 6336 22 micropitting calculations*, *Proceedings of the NREL/CP 5000 77731*, 2020.
- [14]. McCormick M., *Scuffing*, *Gear Solutions Magazine*, Retrieved from <https://gearsolutions.com>, 2016.
- [15]. Gurau L., *Failure Case Study Series Part One: Analysis of Oxygen Compressor Shaft Breakage*, *The Annals of "Dunarea de Jos" University of Galati. Fascicle IX, Metallurgy and Materials Science*, vol. 49, no. 1, p. 11-18, 2026.